IEEE Access
Multidisciplinary | Rapid Review | Open Access Journal

Received December 10, 2018, accepted January 14, 2019, date of publication January 22, 2019, date of current version February 6, 2019.

Digital Object Identifier 10.1109/ACCESS.2019.2894219

Directional Modulation Technique for Linear Sparse Arrays

FENG LIU[1], LING WANG[1,2], (Member, IEEE), AND JIAN XIE[1,2], (Member, IEEE)
[1]School of Electronics and Information, Northwestern Polytechnical University, Xi'an 710072, China
[2]Research and Development Institute, Northwestern Polytechnical University, Shenzhen 518057, China

Corresponding author: Jian Xie (xiejian@nwpu.edu.cn)

This work was supported in part by the National Natural Science Foundation of China under Grant 61601372, Grant 61771404, and Grant 61871459, in part by the Shenzhen Science and Technology Innovation Committee of Basic Research Projects under Grant JCYJ20170306154016149 and Grant JCYJ20170815154325384, in part by the China Postdoctoral Science Foundation under Grant 2017M613200, and in part by the Natural Science Basic Research Plan in Shaanxi Province of China under Grant 2017JQ6068.

ABSTRACT As millimeter-wave technology becomes more and more mature, directional modulation (DM) based on large uniform linear arrays, where the adjacent antennas spaced half-wavelength of the frequency of interest, can be realized to ensure the security of millimeter-wave systems. However, for small inter-element spacings, the mutual coupling effects are severe. Therefore, a DM technique using linear sparse arrays (LSAs) is presented to improve spatial resolution and mitigate the effects of mutual coupling. The main idea for DM signal synthesis is to modulate the radiation pattern at the symbol rate by randomly selecting a sparse rate, i.e., a filling fraction, from the given interval $[\alpha_{\min}, \alpha_{\max}]$ and an array formation, i.e., an antenna subset, from the codebook $\mathcal{P}$. This results in a directional radiation pattern that projects a standard constellation in the desired direction and distorted randomized constellations in other directions, which offers security for wireless communication. Numerical comparisons of the symbol error rate performance of the proposed DM technique against conventional array transmission and antenna subset modulation are presented to highlight the advantages of the DM technique for LSAs.

INDEX TERMS Directional modulation (DM), linear sparse array (LSA), sparse rate (SR), array formation (AF), symbol error rate (SER).

I. INTRODUCTION

Information security has been an increasingly critical issue for wireless communications in both civil and military fields due to the broadcast nature of wireless media. The traditional means to guarantee the security of wireless communications is encrypting confidential messages at the higher layers of the protocol stack. However, malicious eavesdroppers can decipher the complex encryption mechanism, capture the encrypted information and then decode it due to the extremely high speed increase in computing capacity of the computer. As a result, researchers have turned their interest towards the lower physical layer security (PHY-security) [1], [2]. PHY-security enables wireless communications to exploit the properties of the physical layer to scramble information content potentially intercepted by eavesdroppers, while simultaneously delivering it to its desired receivers intactly.

Directional modulation (DM), as a promising keyless PHY-security technique that can achieve the above purpose with array antennas, has been widely investigated in recent years. DM is a transmitter-side technology that is capable of projecting a standard constellation along a pre-specified direction while distorting the constellation format in all other directions. The concept of DM was first introduced in [3], and DM structures based on near-field diffraction grating interference effects have been proposed [4], [5]. However, the design process in these cases is complicated because the near-field interactions and their spatially-dependent transformation in the far field are so complex. In [6]–[11], DM architectures composed of actively-driven antenna arrays with reconfigurable phase shifters [6], [9]–[11] or radiators [7], [8] were used for DM synthesis via genetic algorithms (GAs) or particle swarm optimization (PSO). Antenna subset modulation (ASM) was utilized for DM synthesis in [12], and the approach was further developed using the spread-spectrum DM architecture in [13]. In ASM, the radiation pattern is modulated at the desired symbol rate, by randomly selecting an antenna subset to provide a distorted signal constellation in undesired directions, while maintaining a clear constellation in the desired direction. Yuan and Fusco [14], [15] proposed the constrained far-field radiation pattern approach, and the

far-field radiation pattern separation approach was developed. Then, the orthogonal vector approach was proposed in [16] and [17] for the analysis and synthesis of DM transmitters. The linkage between DM and artificial noise (AN) was established in [18] and [19], which provided another perspective for DM synthesis.

However, most existing literature about DM is based on uniform linear arrays (ULAs) with a maximum half-wavelength spacing between adjacent antennas to avoid spatial aliasing. The small carrier wavelength at millimeter wave frequencies enables a large array available in practice [20]. ULAs have been widely adopted in millimeter wave wireless communications. However, it is noted that too small inter-element spacing can cause strong mutual coupling effects and it is not conducive to the correct acquisition of information by desired receivers. Thus, the performance of large arrays is adversely affected.

Compared with the ULA, a linear sparse array (LSA) [21], that is, an antenna array composed of antenna elements extracted from part of a regular ULA, can narrow the scanned beam width with fewer antenna elements, improve the spatial resolution, and weaken the mutual coupling effect between the elements. Therefore, the LSA is more suitable for DM systems than the ULA. Unfortunately, the periodic thinning of the array will cause high sidelobes in the array pattern, which will cause some interference with secure information communication. The utilization of intelligent algorithms such as genetic and simulated annealing algorithms to optimize the LSA structure can only suppress the sidelobes' levels, but eavesdroppers in undesired directions with receivers sensitive enough can still intercept the confidential information from the sidelobes. Therefore, it does not completely meet the security needs of wireless communications.

In this paper, we will focus on DM synthesis primarily for LSAs. The core idea is the randomness of LSAs' selection for different symbols. Randomness is reflected in two aspects. One is the random selection of the sparse rate (SR), and the other is the random selection of array formation (AF). In particular, the determination of the range of sparse rate and generation of the codebook $\mathcal{P}$ for formation selection is described in detail.

The remaining part of this paper is structured as follows. A detailed description of the ULA and LSA transmission models is given in Section II. The principle of the directional modulation technique using LSAs is presented in Section III. Then, Section IV provides simulation results and discussions. Finally, Section V concludes the paper.

Throughout the paper, the following notations will be used: $(\cdot)^T$ and $(\cdot)^H$ designate transpose and complex conjugate transpose, respectively; $\lceil\cdot\rceil$ denotes mapping a real number x to the smallest integer greater than or equal to x; $\max(\cdot)$ and $\min(\cdot)$ denote maximum operation and minimum operation, respectively; $|\cdot|$ represents modulus; Operator "$\circ$" denotes the Hadamard product of two vectors.

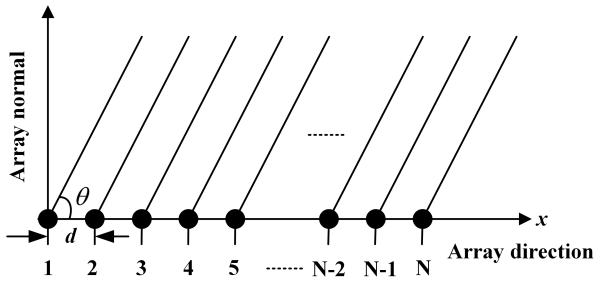

FIGURE 1. Structure of a ULA.

II. SYSTEM MODEL

A. ULA TRANSMISSION MODEL

A multiple-input single-output (MISO) communication system with N transmitting antennas and a single receiving antenna is adopted. However, the ideas proposed in this paper can be extended to multiple receive antennas. We first consider ULAs equipped with omnidirectional antennas, as shown in Fig. 1, although our approach works for uniform planar arrays and uniform cylindrical arrays, i.e., 2D/3D multidimensional periodic arrays. We deploy an N-element ULA with a half-wavelength spacing along the x-axis and with the array centered at the origin. The angular location of the receivers is only specified by the azimuth angle (θ), because the linear array positioned on the x-y plane cannot resolve elevation (ϕ). The transmitter knows the angular location of the desired receiver, but not of the potential eavesdroppers.

Without loss of generality, assuming a narrow-band channel with perfect synchronization and symbol-rate sampling, the received signal at discrete time k along with any direction angle θ can be expressed as

$$y(k,\theta) = \boldsymbol{h}^H(\theta)\boldsymbol{w}(\theta)x(k) + \omega(k), \tag{1}$$

where $\boldsymbol{h}(\theta)$ and $\boldsymbol{w}(\theta)$ are $N \times 1$ channel vector and beamforming vector, respectively. $x(k)$ is the transmitted modulation signal, and $\omega(k)$ is the normalized additive white Gauss noise (AWGN) with zero mean and σ_ω^2 variance, i.e., $\omega \sim \mathcal{CN}(0, \sigma_\omega^2)$. The channel vector, $\boldsymbol{h}(\theta)$, is a function of the receiver's angular location. Generally, in order to avoid spatial aliasing, the maximum spacing between adjacent antennas is set to half a wavelength of the frequency of interest. The normalized channel vector for a receiver located along the θ direction can be written as

$$\boldsymbol{h}(\theta) = \frac{1}{\sqrt{N}}\left[\underbrace{e^{j2\pi\phi_\theta(1)}}_{h_1(\theta)}, \ldots, \underbrace{e^{j2\pi\phi_\theta(n)}}_{h_n(\theta)}, \ldots, \underbrace{e^{j2\pi\phi_\theta(N)}}_{h_N(\theta)}\right]^H, \tag{2}$$

where $\phi_\theta(n)$ is defined as

$$\phi_\theta(n) = \frac{(1-n)d\cos\theta}{\lambda} \quad (n = 1, 2, \ldots, N). \tag{3}$$

Here, d represents the inter-element spacing and λ is the free-space wavelength.

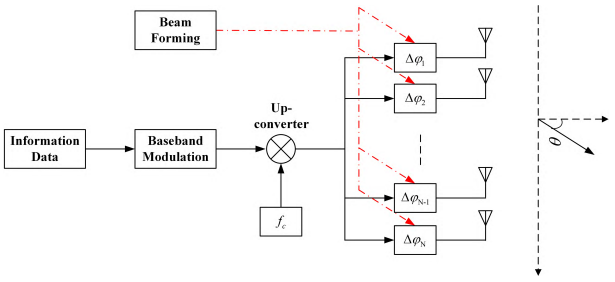

FIGURE 2. A typical phased ULA transmitter.

For ULA mentioned above, Eq. (3) can be simplified to

$$\phi_\theta(n) = \frac{(1-n)\cos\theta}{2} \quad (n = 1, 2, \ldots, N). \tag{4}$$

For linear arrays with variable inter-element spacings, Eq. (3) is replaced by

$$\phi_\theta(n) = \frac{d_n \cos\theta}{\lambda} \quad (n = 1, 2, ..., N). \tag{5}$$

where d_n is the distance from element n to the first element. This is a typical non-grid array. Limited to the length of the article, we only consider grid arrays for the sake of the present discussion.

Fig. 2 shows a block diagram of a typical phased ULA transmitter whose modulation is generated in the baseband, and then followed by RF up-conversion and beamforming in the RF domain. Finally, the phase-shifted signal at each branch is amplified by a power amplifier (PA) before going into the antenna elements.

M-ary phase shift keying (MPSK) modulation will be used by the transmitter. Then, the complex phase-modulated symbol is given by

$$x(k) = \sqrt{P}e^{j\psi(k,l)} = \sqrt{P}e^{j2\pi(l-1)/M}, \ l = 1, 2, \ldots, M. \tag{6}$$

where P denotes the transmission power.

Let θ_d and θ_u denote, respectively, the desired radial and undesired direction. As a side note, the transmitter knows θ_d but not θ_u. In order to orient the main beam towards the desired direction θ_d, the beamforming vector,$\boldsymbol{w}(\theta)$, is set as

$$\boldsymbol{w}(\theta) = \boldsymbol{h}(\theta_d), \quad \forall k. \tag{7}$$

Recalling Eq. (1), in an arbitrary direction θ, the received symbol is given by

$$y(k, \theta) = \boldsymbol{h}^H(\theta)\boldsymbol{h}(\theta_d)\sqrt{P}e^{j\psi(k,l)} + \omega(k). \tag{8}$$

Then, substituting Eq. (3) into Eq. (8), ignoring the noise, and letting $\xi_\theta = \frac{\pi d}{\lambda}(\cos\theta - \cos\theta_d)$, we have

$$\begin{aligned} y(k, \theta) &= \sqrt{P}e^{j\psi(k,l)}e^{-j(N+1)\xi_\theta} \cdot \frac{1}{N}\sum_{n=1}^{N} e^{jn2\xi_\theta} \\ &= \sqrt{P}e^{j\psi(k,l)}\frac{\sin(N\xi_\theta)}{N \cdot \sin(\xi_\theta)} \\ &= \zeta(\theta)x(k), \end{aligned} \tag{9}$$

where $\zeta(\theta) = \frac{\sin(N\xi_\theta)}{N\cdot\sin(\xi_\theta)}$ is a real scaling factor for every θ.

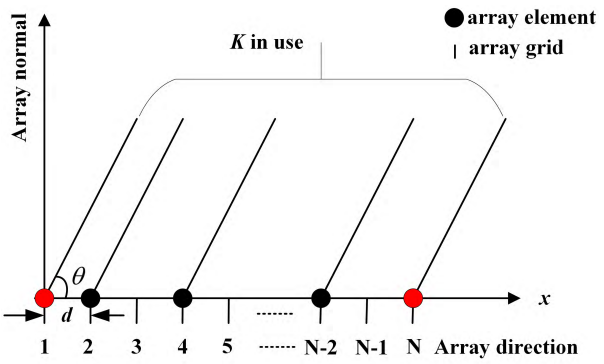

FIGURE 3. Structure of a grid LSA.

It is noted that the k-th received datum is equal to the symbol $x(k)$ if and only if the target receiver detects transmissions from the desired direction θ_d, which means that $\theta = \theta_d$, and $\zeta(\theta)$ reaches its maximum value, i.e., $\zeta(\theta) = 1$.

It is not difficult to see from Eq. (9) that the disadvantage of the traditional phased ULA transmission technique is that there are only differences in amplitude of the received signals in different directions, while the constellations of modulated signals received at different positions are the same, i.e., the relative phase relationship between the constellation points does not change. Therefore, as long as the eavesdroppers have sufficiently sensitive receivers, they can still successfully capture correct information, which undoubtedly affects the security of wireless communications.

B. LSA TRANSMISSION MODEL

A small carrier wavelength at millimeter wave frequencies enables an array to accommodate a large number of antennas. At the same time, the antenna elements become smaller and cheaper. However, the high cost of an entire front-end per antenna makes a large array very expensive, as in the case of a phased array radar with hundreds of antennas. As a result, the benefits afforded by using more front-ends are only gained at the cost of increasingly complex and expensive hardware. Therefore, the thinning of large arrays is becoming increasingly desirable.

In this paper, grid LSAs are considered only for the sake of analysis. A grid LSA refers to an antenna array formed by extracting a portion of the elements of a ULA with an inter-element spacing d according to the given optimization criteria.

In Fig. 3, we consider a K-element LSA obtained from an N-element ULA with all elements spaced $d = \lambda/2$ apart. The SR of the sparse array, i.e., the filling fraction, is defined as

$$\alpha = \frac{K}{N} \times 100\%. \tag{10}$$

The ULA serves as a reference for comparison with the LSA because a LSA is obtained by extracting some elements from a ULA. That is to say, elements in ULA are made active or inactive to form a LSA by reducing the sidelobe

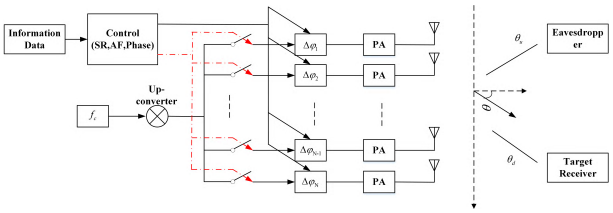

FIGURE 4. A DM transmitter for grid LSA.

level. Here, a binary digit, i.e., a bit a_n is used to indicate whether the nth element is excited or not. An active element corresponds to one, while an inactive element corresponds to zero

$$a_n = \begin{cases} 1, & \textit{active element} \\ 0, & \textit{inactive element}. \end{cases} \tag{11}$$

Therefore, we use an $N \times 1$ vector to denote an array formation. The nth element of $\boldsymbol{a} = [a_1, a_2, \ldots, a_N]$ is defined in Eq. (11).

In this investigation, all arrays synthesized will contain a fixed outermost element pair. The purpose of fixing the outermost pair is to ensure a specific aperture size,$L = (N-1)\times d$, as a basis for comparison. If the SR is unchanged during the sparsing process, the number of active array elements is a fixed number K.

The system architecture of a DM transmitter for LSA is shown in Fig. 4. A fundamental difference between the method proposed in this paper and conventional phased ULA transmitters is that modulation occurs in the RF domain. For each symbol transmitting, there are only K active antennas, so the RF chains subset used for transmission of each symbol contains exactly K RF chains. It is noted that K is a random integer for every symbol. The control block selects the subset of K active antennas using a high-speed RF switch and then determines the phase shifts for each antenna in use. We will demonstrate the scheme for a random selection of SR and AF and the method for DM signal synthesis for secure transmissions in the following part.

Since there is no baseband modulation involved, $x(k) = \sqrt{P}$ denotes the constant amplitude carrier. The effects of data modulation, beamforming and AF selection for the transmitting symbol at discrete time k are succinctly represented by the beamforming vector,$\boldsymbol{w}(k, \theta)$, for LSAs,

$$\boldsymbol{w}(k, \theta) = [\boldsymbol{a}(k) \circ \boldsymbol{h}(\theta_d)]e^{j\varphi(k)}, \tag{12}$$

where $\varphi(k)$ is a data-dependent phase offset introduced in addition to the progressive inter-antenna phase shifts.

Without loss of generality, assuming a narrow-band channel with perfect synchronization and symbol-rate sampling, the received signal at discrete time k along any direction angle θ can be written as

$$\begin{aligned} y(k, \theta) &= \boldsymbol{h}^H(\theta)\boldsymbol{w}(k, \theta)x(k) + \omega(k) \\ &= \boldsymbol{h}^H(\theta)[\boldsymbol{a}(k) \circ \boldsymbol{h}(\theta_d)] \cdot \sqrt{P}e^{j\varphi(k)} + \omega(k). \end{aligned} \tag{13}$$

The scaling factor $\zeta(\theta, \boldsymbol{a})$ is defined as

$$\zeta(\theta, \boldsymbol{a}) = \boldsymbol{h}^H(\theta)[\boldsymbol{a}(k) \circ \boldsymbol{h}(\theta_d)]. \tag{14}$$

Then, substituting Eq. (14) into Eq. (13) and ignoring noise for the convenience of analysis, we have

$$y(k, \theta) = \underbrace{\zeta(\theta, \boldsymbol{a})}_{scalar} \cdot \underbrace{\sqrt{P}e^{j\varphi(k)}}_{information}, \tag{15}$$

where the scaling factor $\zeta(\theta, \boldsymbol{a})$ is a complex number for every $\theta \neq \theta_d$ and changes with different symbols. When $\theta = \theta_d$, i.e., $\zeta(\theta, \boldsymbol{a}) = 1$, we obtain the noiseless received signal using

$$y(k, \theta) = \sqrt{P}e^{j\varphi(k)}. \tag{16}$$

This indicates that the constellation received in the desired direction remains the same as the information delivered.

When $\theta \neq \theta_d$, let $\zeta(\theta, \boldsymbol{a}) = \delta(\theta, \boldsymbol{a}) \cdot e^{j\Delta\varphi(\theta, \boldsymbol{a})}$, we have

$$y(k, \theta) = \delta(\theta, \boldsymbol{a}) \cdot \sqrt{P}e^{j\varphi(k)} \cdot e^{j\Delta\varphi(\theta, \boldsymbol{a})}. \tag{17}$$

It is easy to see that the signal received is not only related to the direction θ, but also to the AF of the LSA, $\boldsymbol{a}$. There exists a random amplitude difference $\delta(\theta, \boldsymbol{a})$ and a random phase difference $\Delta\varphi(\theta, \boldsymbol{a})$ between the received signal and the original signal for each symbol, which disrupts the constellation format received in undesired directions at random. The proposed method offers security through the transmission of digitally modulated information along *a prior* assigned direction, while simultaneously distorting the constellation formats of the same signal in all other directions. Therefore, it inhibits eavesdroppers from demodulating the useful information without knowing the intended direction, thus enhancing the security of the system.

III. PRINCIPLES OF DM TECHNIQUE FOR LSAS

The directional modulation technology proposed by Daly and Bernhard [6], which controls transmitted signals by adjusting the phased array phase shifter, scrambles the constellation in the undesired directions. However, there is a certain regularity in the disturbances introduced which makes the method not secure enough. Direction modulation can also achieve the purpose of disturbing the constellation through the selection of an antenna subset for signal transmission, called antenna subset modulation (ASM), and was studied by Valliappan *et al.* [12]. This method can interfere with the reception of signals by eavesdroppers without affecting legitimate receivers. However, it only considers the different array formations for a fixed number of antennas, and the DM signal synthesis is not included.

In order to reinforce the security of wireless information transmission, a DM technique for LSAs is proposed. The method can be considered as an extension to some extent. The essence of the method proposed lies within two aspects of randomness for a LSA selection for every transmitted symbol. One is the randomness of the sparse rate selection, which occurs at symbol level. The other is the randomness of the antenna subset selection after the sparse rate has been

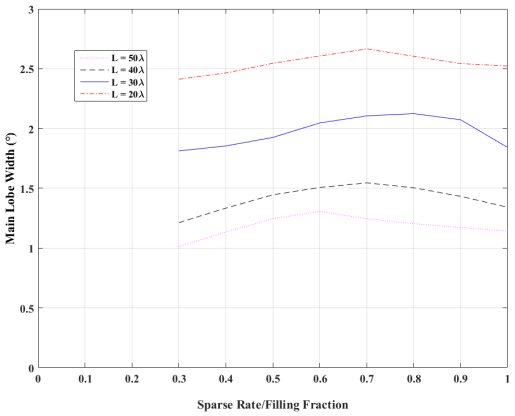

FIGURE 5. Main lobe width for various apertures and sparse rate.

selected, which occurs at the RF chain. It is noted that for each transmitted symbol, only one LSA is utilized. That is to say, the LSA in use is one randomly selected subset from the total antenna set for the randomly selected value of sparse rate.

When transmitting a symbol, at first, we randomly generate an SR (α), then sparse the N-element ULA according to the value of α. That is, the sinusoidal carrier signal drives only $\lceil N\alpha \rceil$ antennas after passing through phase shifters and PAs. The primary task to achieve secure transmission is to construct a LSA set as a codebook. Then, we randomly select an AF from the codebook to synthesize the DM signal.

In the following, the random selection of a sparse rate and an array formation is discussed in detail.

A. RANDOM SPARSE RATE SELECTION

First, we investigate what level of thinning will produce the best results considering the characteristics of the LSAs. Then, we will give the value range of the sparse rate. Finally, a sparse rate is randomly selected from the SR set $\mathcal{J}$.

As is known, if a DM signal has a narrower main lobe beamwidth (3-dB beamwidth) and a lower peak sidelobe level (PSL), it will offer better physical layer performance with regard to security.

The beamwidth of the main lobe is rather insensitive to changes of the element positions and to the total number of elements, and depends primarily on the total length of the array. Unless the excitations of the elements are strongly tapered and the inter-element spacings vary wildly, the following equation can be used with reasonable accuracy to determine the total aperture length L of a broadside array required to produce a 3-dB beamwidth $\Delta\theta$, where it is assumed that $\Delta\theta \ll 1$ radian

$$\frac{L}{\lambda} \approx \frac{1}{\Delta\theta}. \tag{18}$$

Observing Eq. (18), it is apparent that a broadside array with a narrower 3-dB beamwidth needs a larger aperture L. That is, a large array is beneficial to the security of DM techniques.

We have investigated the relationship between the thinning levels and the main lobe width for various apertures as shown in Fig. 5. The main lobe width is plotted for four different apertures filled to various extents. All apertures ranging from 20λ to 50λ exhibit similar behavior. As can be seen in the figure, as the sparse rate increases, the main lobe width increases as well. However, when the sparse rate is increased to a certain ratio, the main lobe width is no longer significantly broadened. For the same aperture, the main lobe width changes slightly for different filling fractions. So, the fact that the beamwidth of the main lobe depends primarily on the total aperture of the array has been validated. In practice, we choose the fixed aperture to be as large as possible.

To exploit the additional degrees of freedom (DOF) provided in the spatial domain, the thinning of a large array with the same aperture can be employed for more effective DM. Large broadside arrays with variable inter-element spacings are of great importance when the average spacing is larger. For such arrays, the number of elements used in conventional arrays to obtain given directional characteristics can be markedly reduced in order to reduce costs. Therefore, only arrays with large average inter-element spacings will be considered. Because the elements are assumed to be spaced much more than one wavelength apart, the achievable sidelobe level is expected to have a lower limit. This can perhaps be best understood by considering a broadside array of equidistant omnidirectional elements. To avoid strong grating lobes in the radiation pattern, the spacing between neighboring elements must be smaller than about one wavelength. If the spacing in the equispaced broadside array is allowed to exceed one wavelength, the width of the main beam becomes smaller. However, at the same time a number of grating lobes with the same level as the main lobe appears. These grating lobes can be suppressed to some extent without influencing the width of the main beam appreciably by suitably rearranging the elements of the array. However, the lobes outside the main beam cannot be suppressed to an arbitrarily low level. The lowest obtainable sidelobe level depends on the number of elements used in the array; the larger the number of elements, the lower the theoretical limit of the sidelobe level. This limit can be predicted very easily for the case of a very large array. For such arrays, the width of the main lobe depends essentially upon the length of the array and only slightly on the number of elements in the array and on the way the elements have been arranged. When all elements are given the same excitation, and the mutual couplings are neglected, the array gain equals the number of array elements.

In a study by Andreasen [23], a lower bound to the peak sidelobe level (PSL) was determined. This lower bound is given by

$$PSL(N, d_{av}) = -10\log(N/2) - 10\log(\frac{1}{1-\lambda/2d_{av}})\ dB. \tag{19}$$

Eq. (19) is based on a given number of elements N and a given average inter-element spacing d_{av}, but it is designed for use on large arrays. The nature of this function makes it inaccurate when d_{av} is close to $\lambda/2$, and this inaccuracy

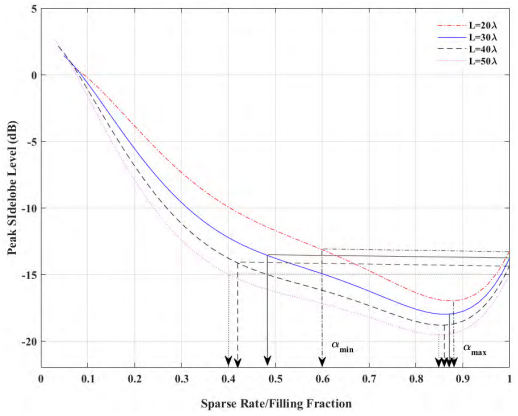

FIGURE 6. Peak sidelobe levels for various apertures and sparse rate.

implies that the least amount of thinning is best. That is, there exists a sparse rate to make the PSL minimum.

In Fig. 6, the PSL is plotted for four different apertures filled to various extents. All apertures ranging from 20λ to 50λ exhibit similar behavior. As we can see, the lowest possible PSL is achieved when 85% - 87% of the available elements are used. When apertures are 20% - 80% filled, a roughly linear relationship between PSL and amount of thinning is seen.

As discussed above, when the radiated energy is constant, the main lobe width and the peak sidelobe level are correlated. The main lobe width increases and the peak side lobe level is correspondingly lowered. Also, the main lobe width is insensitive to changes of the element positions and to the total number of active elements. Therefore, in order to ensure that the sparse array maintains a narrow main lobe width, it is necessary to maintain the sparse array with the largest aperture size and thus keep the outermost element pair active. A reasonable distribution of active elements is then selected for the middle part to suppress the peak sidelobe level.

According to Eq. (19), when the aperture of the array is fixed, the PSL depends primarily on the average inter-element spacing d_{av}. That is, the PSL depends primarily on the number of active elements, K, and a lower PSL makes a hard task for an eavesdropper to demodulate the useful information. Therefore, the values of K are taken according to the PSL. As shown in Fig. 6, when the PSL reaches its minimum, the corresponding sparse rate α is denoted by $\alpha_{\max}$. When all elements are active in the array, the value of the PSL is denoted by PSL_{full}. When the PSL reaches PSL_{full}, the corresponding sparse rate α is denoted by $\alpha_{\min}$($\alpha_{\min} \neq 1$). Then, the SR set $\mathcal{J}$ is given by

$$\mathcal{J} = \{\alpha \in R \mid \alpha_{\min} \leq \alpha \leq \alpha_{\max}\}. \tag{20}$$

The parameter $\alpha_{\min}$ is chosen to utilize as few RF chains as possible to save costs and to increase the difficulty for eavesdroppers demodulating with lower PSL, whereas $\alpha_{\max}$ is chosen to maintain the PSL as low as in the case of the full array.

The sparse rate chosen for a particular symbol is equally likely to be any value from the set $\mathcal{J}$. Similarly, the values of K can be randomly taken from the set $\mathcal{K}$

$$\mathcal{K} = \{K \in Z \mid \lceil N\alpha_{\min} \rceil \leq K \leq \lceil N\alpha_{\max} \rceil\}. \tag{21}$$

B. RANDOM ARRAY FORMATION SELECTION

In what follows, the LSA in Fig. 3 is analyzed from the aspect of radiation pattern. In a study by Mailloux [22], the far-field radiation pattern of a K-element LSA excited by equal current amplitudes at arbitrary discrete time k and along any direction θ can be expressed as

$$F(k,\theta) = \sum_{n=1}^{N} f_n(k,\theta) a_n e^{-j\gamma} \cdot e^{j\pi(1-n)\cos\theta}, \tag{22}$$

where $f_n(k,\theta)$ is the pattern of element n, and for an isotropic antenna, $f_n(k,\theta) = 1, \forall n$, while γ denotes the phase weighting of the nth element. As defined in Eq. (11), a_n denotes whether the nth element is excited or not, satisfying

$$\begin{cases} a_1 = a_N = 1 \\ a_n \cdot (a_n - 1) = 0, \quad n = 1, 2, ..., N \\ \boldsymbol{a}^T \boldsymbol{a} = K. \end{cases} \tag{23}$$

When the main beam direction is the desired direction θ_d, we have

$$\gamma = \frac{2\pi}{\lambda}(1-n)d\cos\theta_d = \pi(1-n)\cos\theta_d. \tag{24}$$

Substituting Eq. (24) into Eq. (22), we have

$$F(k,\theta) = \sum_{n=1}^{N} a_n e^{j\pi(1-n)(\cos\theta - \cos\theta_d)}. \tag{25}$$

Then, the PSL of pattern for the K-element LSA is given by

$$PSL = \max_{\theta \in S}(F_{dB}(k,\theta)) = \max_{\theta \in S}\left(\frac{F(k,\theta)}{\max(F(k,\theta))}\right), \tag{26}$$

where $F_{dB}(k,\theta)$ denotes the normalized pattern function and S denotes the sidelobe range of the pattern.

Because the main lobe 3dB-width of the pattern is $\Delta\theta$, we have

$$S = \left\{\theta \mid \theta_{\min} \leq \theta \leq \theta_d - \Delta\theta/2 \cup \theta_d + \Delta\theta/2 \leq \theta \leq \theta_{\max}\right\}. \tag{27}$$

For the N-element array, the number of subsets with K active antennas is $\binom{N-2}{K-2} = \frac{(N-2)!}{(K-2)!(N-K)!}$. Even for moderate values of N and K, this number can be enormous; for $N = 51$, and $K = 25$, $\binom{N-2}{K-2} \approx 5.8 \times 10^{13}$. Obviously, when the number of active antennas is changing with each symbol, our codebook $\mathcal{P}$ is almost $\sum_{i=0}^{\lceil N\alpha_{\max}\rceil - \lceil N\alpha_{\min}\rceil} \binom{N-2}{\lceil N\alpha_{\min}\rceil + i - 2} / \binom{N}{K}$ times that of the ASM method. This facilitates the randomization in phase, which is the improvement in our method.

Given the impracticality of an exhaustive search, heuristic optimization techniques based on genetic algorithms are utilized for optimized antenna subset selection. We focus on genetic algorithms to find a codebook of antenna subsets that have a lower PSL, as this will benefit security. While the amplitude of the received symbols in undesired directions is now lower, the randomization in phase caused by the antenna subset selection is preserved by the use of a large enough codebook.

The optimization goal is to find an optimized solution of the AF, $\boldsymbol{a}$, to minimize the PSL. Then, the optimization problem can be written as

$$\begin{aligned} &\min_{a} (PSL) \\ &s.t.\ \ a_1 = a_N = 1 \\ &\qquad a_n \cdot (a_n - 1) = 0,\ \ n = 1, 2, \ldots, N \\ &\qquad \mathbf{a}^T \mathbf{a} = K. \end{aligned} \tag{28}$$

This is an optimization problem with a constraint given by integer nonlinear equality.

A genetic algorithm is a global intelligent stochastic optimization algorithm with the characteristic of intelligence, self-organization and self-adaptation, and is therefore, suitable for this application. Because the number of possible subsets is large enough, we can obtain a sufficient collection of array configurations with similar sidelobe properties after multiple runs of the GA. The random initialization and the probabilistic nature of the genetic algorithm ensure that we do not converge to the same local optimum after each run. Thus, the arrays synthesized are stacked to form the AF codebook $\mathcal{P}$. Next, we choose an AF at random from the codebook $\mathcal{P}$ for the synthesis of the DM signal.

C. DM SIGNAL SYNTHESIS

Note that the AF selection is only to reduce the peak sidelobe level as the optimization goal. However, it does not consider the degree of distortion of the constellation in undesired directions. Hence, that may not be strict enough for achieving safe wireless transmission. Once the AF has been selected, we take this fact into account for DM signal synthesis to enhance the security of information transmission.

Let us assume that the transmitter uses the LSAs mentioned above and communicates with the MPSK signal described by Eq. (6).

From the signal processing perspective, $F(k, \theta)$ in Eq. (24), as a complex digital symbol with a magnitude and a phase, and can thus be regarded as a constellation point in IQ space. For the convenience of analysis, the far-field radiation pattern for the lth symbol is rewritten as

$$F_l(\theta) = \sum_{n=1}^{N} a_n e^{j\pi(1-n)\cos\theta} \cdot e^{-j\gamma_{ln}}. \tag{29}$$

In order to ensure that the intended receivers can recover information correctly, we attempt to minimize a cost function given by

$$\begin{aligned} \Lambda_1 = &\sum_{l=1}^{M} |F_l(\theta_d) - x(k, l)| \\ &-\pi \le \gamma_{ln} \le \pi,\ \ l = 1, 2, \ldots, M;\ \ n = 1, 2, .., N \end{aligned} \tag{30}$$

At the same time, to generate the maximally distorted constellation diagram in undesired directions, we try to maximize a cost function which is defined as

$$\begin{aligned} \Lambda_2 = &\sum_{l=0}^{M-1} \sum_{k=0, k\neq \frac{\Delta\theta}{2step}}^{\frac{\Delta\theta}{step}} \left| F_l(\theta_d - \Delta\theta/2 + step \times k) - x(k, l) \right| \\ &-\pi \le \gamma_{ln} \le \pi,\ \ l = 1, 2, \ldots, M;\ \ n = 1, 2, .., N \end{aligned} \tag{31}$$

where $\Delta\theta$ is a constant associated with the 3dB main lobe beam width, while *step* is the step size of azimuth angle. The symbol error rate (SER) performance of receivers varies tremendously near $\theta_d - \Delta\theta/2$ and $\theta_d + \Delta\theta/2$. The stepping azimuth angle is usually set to 0.1°.

Therefore, a multi-objective optimization model for DM signal synthesis can be designed as follows

$$\begin{aligned} &\min \Lambda_1 \\ &\max \Lambda_2 \\ &s.t.\ -\pi \le \gamma_{ln} \le \pi, \\ &\qquad -\pi \le \gamma_{ln} \le \pi,\ \ l = 1, 2, \ldots, M;\ \ n = 1, 2, .., N \end{aligned} \tag{32}$$

The optimization goal is to find an optimized solution of γ_{ln} to achieve DM. It is easy to use a multi-objective GA to solve the problem.

In summary, the process of the DM technique for LSAs is shown in Table 1.

TABLE 1. DM technique process for LSAs.

Operation steps	Content
Step 1	For each symbol, randomly select a SR from the set $\mathcal{J}$ to obtain the total antenna number in use using $K = \lceil N\alpha \rceil$
Step 2	Obtain the codebook $\mathcal{P}$ through (28)
Step 3	Select an AF from the codebook $\mathcal{P}$ at random
Step 4	Calculate a set of phase shifts for every symbol using (32) to synthesize the DM signal.

IV. SIMULATION RESULTS AND DISCUSSIONS

In this section, we discuss several simulations to demonstrate the proposed method and compare its performance with conventional array transmission and antenna subset modulation transmission.

We assume that the modulated signal uses Gray-coded QPSK and the AWGN power is the same for all directions.

For the sake of brevity, we initially consider to thin a ULA, which will result in a change of element spacing. So, it is

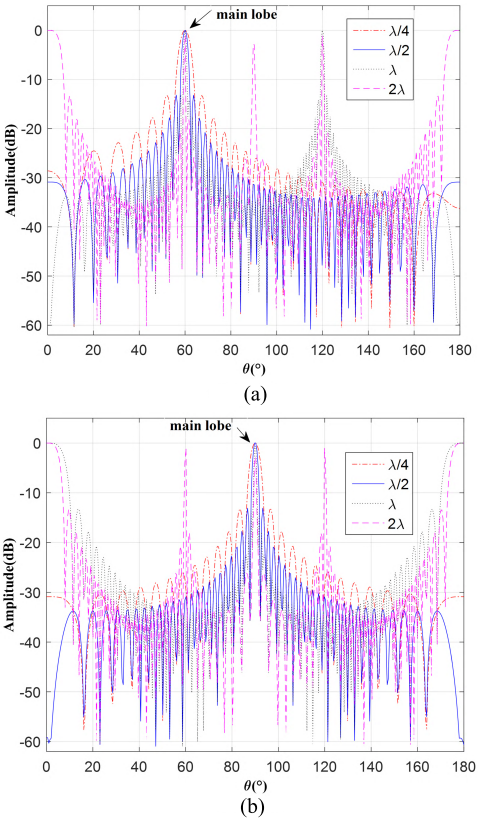

FIGURE 7. Normalized radiation patterns for 50-element ULAs with four different inter-element spacings.

necessary to first analyze the influence of the element spacing variation on the array pattern.

A ULA with inter-element spacing not more than half-wavelength is called a standard array, while a ULA with inter-element spacing greater than half-wavelength is called a sparse array. If there are multiple peaks in the visual range of beam aliasing, the peak in the main direction is called the main lobe, while peaks in other directions are called grating lobes. From the spatial sampling perspective, a standard array is over-sampling. There is only one peak in the visual range, i.e., a standard array has no grating lobes. A sparse array is under-sampling. Since the spatial sampling theorem is not satisfied, there are multiple peaks in this range, and therefore a sparse array produces grating lobes.

Fig. 7 shows the normalized radiation patterns for ULAs with four inter-element spacings, $\lambda/4$, $\lambda/2$, λ and 2λ respectively. The arrays with inter-element spacings $\lambda/4$ and $\lambda/2$ have only one main lobe. When the inter-element spacing is equal to λ, two grating lobes and one main lobe appear. When the inter-element spacing is 2λ, there are four grating lobes and one main lobe, which do not change with the array orientation. Additionally, it can also be clearly seen that when the number of array elements is constant, the greater the inter-element spacing is, the smaller the width of the main lobe is, and the higher the resolution is. The smaller main lobe width enhances security, while the grating lobe effect is not good for legitimate users.

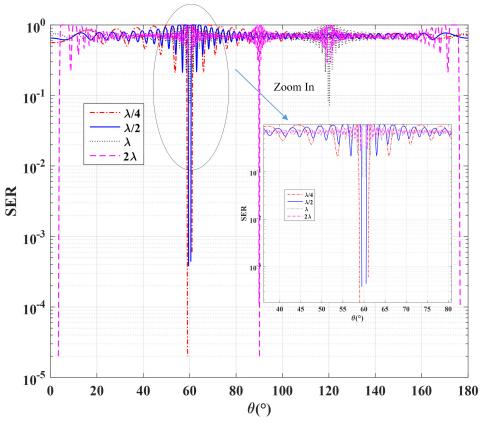

FIGURE 8. SER curve for 50-element ULAs with four inter-element spacings.

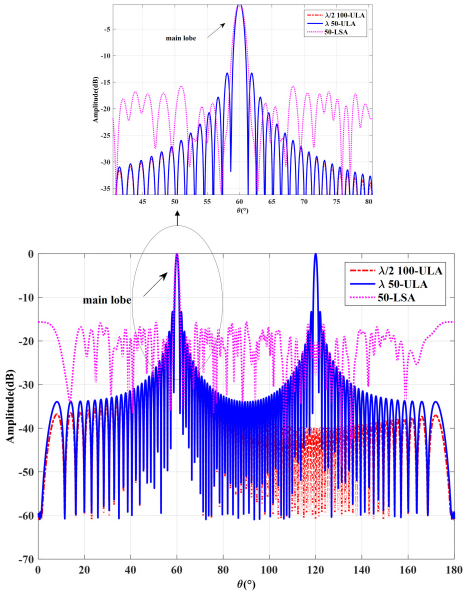

FIGURE 9. Normalized radiation patterns for the LSA ($\alpha = 0.5$), 50-element ULA, and 100-element ULA (all with the same aperture about 50λ).

Ideally, the desired receiver can demodulate the signal without errors, while the SER in all other directions should be as high as possible. Next, sparse arrays are applied to conventional array transmission and the security performance is analyzed according to the SER at the receiving end. Apart from the different inter-element spacings, the rest of the simulation conditions are the same. The resulting SER curve is shown in Fig. 8.

In Fig. 8, the SER curves still follow the periodicity. The sparse array with an element spacing of 2λ has a main lobe nulling, i.e., nulling in desired direction, which is what we expected. There are also nulls at four other angles, coinciding with the sidelobe positions of the pattern. The arrays with other inter-element spacings exhibit behavior similar to the normalized radiation pattern in Fig. 7. Therefore, only the

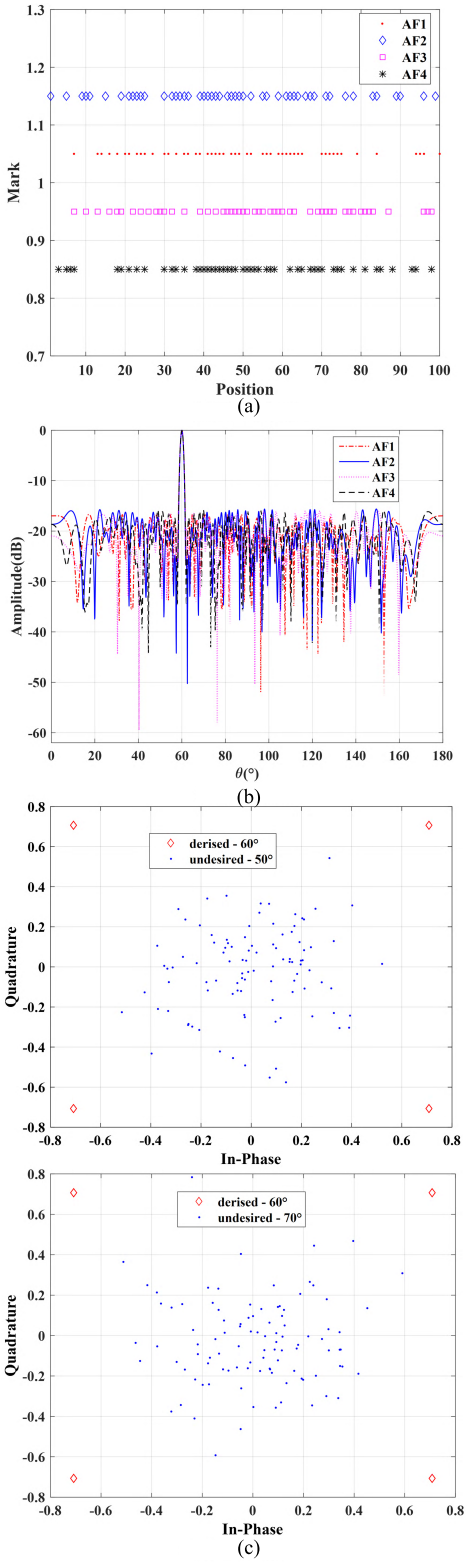

FIGURE 10. (a) Element location, (b) Beam Patterns and (c) Constellations for DM signal when SR is fixed to 0.5 with four different AFs.

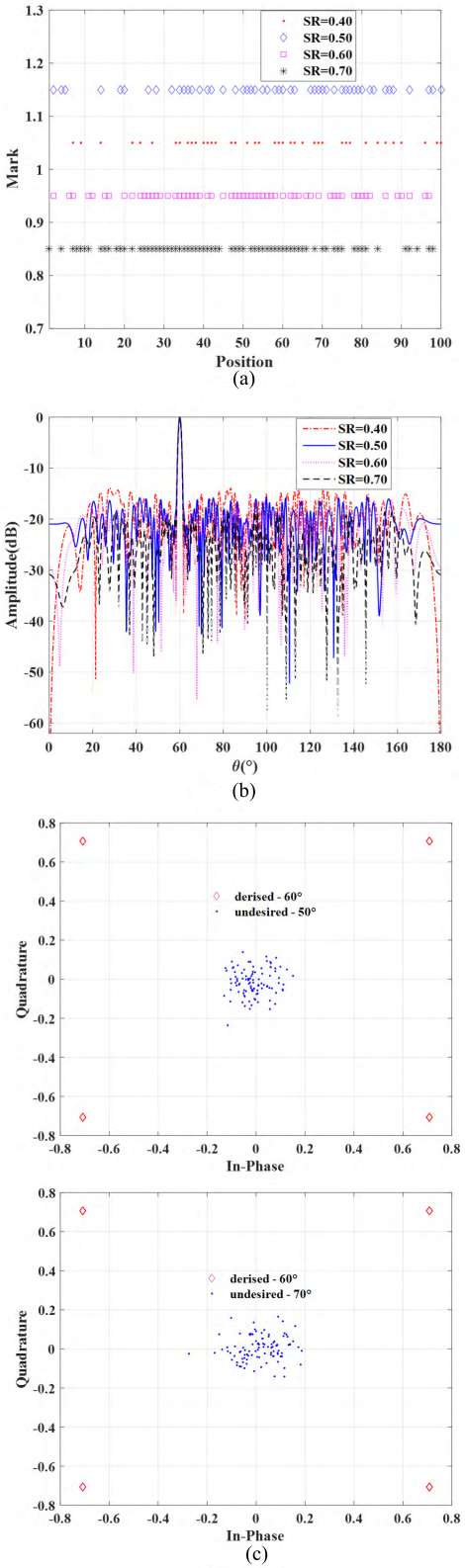

FIGURE 11. (a) Element positions, (b) normalized radiation patterns and (c) Constellations for LSAs with different SRs.

pattern is analyzed and the SER curves are given in the following part. SER nulling in undesired directions is collectively called as the SER grating lobe.

LSA grating lobes are a significant drawback. However, when the number of array elements is constant, the greater the inter-element spacing is, the narrower the SER nulling

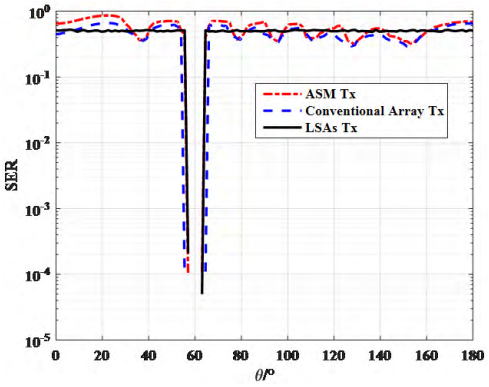

FIGURE 12. SER curves for conventional phased array, ASM and LSAs transmission.

of the main lobe is. In the sidelobe region, the performance difference of SERs with different arrays is very small, and the volatility is not significant. Hence, LSAs are more secure than standard arrays, provided that the grating lobes are eliminated. In the following, we assume that the sparse rate is fixed at 50%. Firstly, to compare the differences between the LSA, the N-element ULA and the $N/2$-element ULA (keeping the same aperture), the corresponding patterns are shown in Fig. 9. Secondly, to compare the differences between three different array formations from codebook $\mathcal{P}$, the simulation results are shown in Fig. 10.

In Fig. 9, from the perspective of the main lobe width, the LSAs achieve a slightly wider main lobe width using half the elements compared with the 100-element ULA. Moreover, with the same aperture, the LSAs solve the problem of periodic grating lobes appearing when the element spacing is greater than $\lambda/2$ compared with the 50-element ULA with a spacing of λ. However, considering the side lobe level of the LSAs is higher than that of the ULAs. Therefore, the LSAs use the higher side lobe to obtain a narrower beam width.

In Fig. 10, we see that the four AFs can synthesize the same constellation as QPSK modulation in the desired direction, while the constellation received by eavesdroppers produces a random deformation. Moreover, the randomness of the AF selection makes the far-field mode along the side lobes constantly change to generate additional constellation points. These extra constellation points disturb those in undesired directions, so eavesdroppers cannot demodulate correctly. Therefore, secure transmission of communication information can be achieved by using the PHY-layer.

Due to the variation of SR at each symbol, the effect of different SRs on array pattern is analyzed as follows. In Fig. 11, different LSAs correspond to different beam patterns. For different SRs, the main lobe remains almost the same, while the side lobes change significantly. This results in random changes in the constellation points for each symbol received in undesired directions, so the constellation restored by eavesdroppers can have aliasing effects. Compared with Fig. 10 (c), it is not difficult to see that as the SR changes, the degree of aliasing of the signal constellation in undesired directions becomes more severe, which increases the difficulty of the eavesdroppers recovering the correct information. Therefore, the security of information transmission is enhanced.

Fig. 12 shows the SER achieved by a conventional phased array, the ASM in [12] and the LSAs. It is evident that the SER beam-width obtained with fewer antennas for LSAs is almost the same as the ASM, and a little narrower than the conventional array. The LSA is also able to produce less notable sidelobes than those obtained for the conventional array or ASM transmission, which leads to enhanced security performance. This is mainly attributed to the randomness of the SR selection and the AF selection.

V. CONCLUSION

In order to enhance the security of the directional modulation technique, we introduce randomness at each symbol for SR selection as well as for the AF selection. Therefore, the constellation point of each symbol received in an undesired direction will produce a random change, so the constellation diagram restored by the eavesdropper suffers from an aliasing effect, which enhances the security of information transmission. The numerical comparisons of the SER performance of the proposed DM technique against conventional array and ASM transmission are presented to highlight the potential of DM for LSAs with fewer antennas to reduce cost. Experimental verification of the method proposed here will be the subject of future work.

ACKNOWLEDGMENT

Feng Liu would like to thank Dr. Wei Zhang for useful discussions. The help of Dr. Yuexian Wang is appreciated. The authors also would like to thank the anonymous reviewers for their valuable comments and suggestions.

REFERENCES

[1] X. Chen, D. W. K. Ng, W. H. Gerstacker, and H.-H. Chen, "A survey on multiple-antenna techniques for physical layer security," *IEEE Commun. Surveys Tuts.*, vol. 19, no. 2, pp. 1027–1053, 2nd Quart., 2016.

[2] F. Shu *et al.*, "Directional modulation-based secure wireless transmission: Basic principles, key techniques, and applications," (in Chinese), *Sci. Sin. Inform.*, vol. 47, no. 9, pp. 1209–1225, Sep. 2017.

[3] A. Babakhani, D. B. Rutledge, and A. Hajimiri, "Transmitter architectures based on near-field direct antenna modulation," *IEEE J. Solid-State Circuits*, vol. 43, no. 12, pp. 2674–2692, Dec. 2008.

[4] A. Babakhani, D. B. Rutledge, and A. Hajimiri, "Near-field direct antenna modulation," *IEEE Microw. Mag.*, vol. 10, no. 1, pp. 36–46, Feb. 2009.

[5] A. H. Chang, A. Babakhani, and A. Hajimiri, "Near-field direct antenna modulation (NFDAM) transmitter at 2.4 GHz," in *Proc. IEEE Antennas Propag. Soc. Int. Symp. (APSURSI)*, Charleston, SC, USA, 2009, pp. 1–4.

[6] M. P. Daly and J. T. Bernhard, "Directional modulation technique for phased arrays," *IEEE Trans. Antennas Propag.*, vol. 57, no. 9, pp. 2633–2640, Sep. 2009.

[7] M. P. Daly, E. L. Daly, and J. T. Bernhard, "Demonstration of directional modulation using a phased array," *IEEE Trans. Antennas Propag.*, vol. 58, no. 5, pp. 1545–1550, May 2010.

[8] M. P. Daly and J. T. Bernhard, "Beamsteering in pattern reconfigurable arrays using directional modulation," *IEEE Trans. Antennas Propag.*, vol. 58, no. 7, pp. 2259–2265, Mar. 2010.

[9] Y. Ding and V. Fusco, "Directional modulation transmitter synthesis using particle swarm optimization," in *Proc. IEEE Loughborough Antennas Propag. Conf. (LAPC)*, Loughborough, U.K., 2014, pp. 500–503.

[10] H. Z. Shi and T. Alan, "Direction dependent antenna modulation using a two element array," in *Proc. IEEE Eur. Conf. Antennas Propag. (EuCAP)*, Rome, Italy, Apr. 2011, pp. 812–815.
[11] H. Z. Shi and T. Alan, "An experimental two element array configured for directional antenna modulation," in *Proc. IEEE Eur. Conf. Antennas Propag. (EuCAP)*, Prague, Czech Republic, Mar. 2012, pp. 1624–1626.
[12] N. Valliappan, A. Lozano, and R. W. Heath, Jr., "Antenna subset modulation for secure millimeter-wave wireless communication," *IEEE Trans. Commun.*, vol. 61, no. 8, pp. 3231–3245, Aug. 2013.
[13] T. Hong, M.-Z. Song, and Y. Liu, "RF directional modulation technique using a switched antenna array for communication and direction-finding applications," *Prog. Electromagn. Res.*, vol. 120, no. 8, pp. 195–213, Jan. 2011.
[14] Y. Ding and V. F. Fusco, "Constraining directional modulation transmitter radiation patterns," *IET Microw., Antennas Propag.*, vol. 8, no. 15, pp. 1408–1415, 2014.
[15] Y. Ding and V. F. Fusco, "Directional modulation far-field pattern separation synthesis approach," *IET Microw. Antennas Propag.*, vol. 9, no. 1, pp. 41–48, Dec. 2014.
[16] Y. Ding and V. F. Fusco, "A vector approach for the analysis and synthesis of directional modulation transmitters," *IEEE Trans. Antennas Propag.*, vol. 62, no. 1, pp. 361–370, Jan. 2013.
[17] Y. Ding and V. Fusco, "Orthogonal vector approach for synthesis of multi-beam directional modulation transmitters," *IEEE Antennas Wireless Propag. Lett.*, vol. 14, pp. 1330–1333, Feb. 2015.
[18] R. Negi and S. Goel, "Secret communication using artificial noise," in *Proc. IEEE Veh. Technol. Conf. (VTC)*, Dallas, TX, USA, Sep. 2005, pp. 1906–1910.
[19] J. Hu, S. Yan, F. Shu, J. Wang, J. Li, and Y. Zhang, "Artificial-noise-aided secure transmission with directional modulation based on random frequency diverse arrays," *IEEE Access*, vol. 5, pp. 1658–1667, 2017.
[20] H. Zhao *et al.*, "28 GHz millimeter wave cellular communication measurements for reflection and penetration loss in and around buildings in New York city," in *Proc. IEEE Int. Conf. Commun. (ICC)*, Budapest, Hungary, Jun. 2013, pp. 5163–5167.
[21] B. Zhang, W. Liu, and X. Gou, "Compressive sensing based sparse antenna array design for directional modulation," *IET Microw. Antennas Propag.*, vol. 11, no. 5, pp. 634–641, Apr. 2017.
[22] R. Mailloux, *Electronically Scanned Arrays*. San Rafael, CA, USA: Morgan & Claypool, 2007.
[23] M. Andreasen, "Linear arrays with variable interelement spacings," *IRE Trans. Antennas Propag.*, vol. 10, no. 2, pp. 137–143, Mar. 1962.

FENG LIU received the B.Sc. and M.Sc. degrees from Northwestern Polytechnical University, China, in 2013 and 2016, respectively. He is currently pursuing the Ph.D. degree with the Department of Information and Communications Engineering, Northwestern Polytechnical University, Xi'an. His research interests include wireless communications, array signal processing, and physical-layer security.

LING WANG received the B.Sc., M.Sc., and Ph.D. degrees in electronic engineering from Xidian University, Xi'an, China, in 1999, 2002, and 2004, respectively. From 2004 to 2007, he was with Siemens and Nokia Siemens Networks. Since 2007, he has been with the School of Electronic and Information, Northwestern Polytechnical University, Xi'an, where he was promoted to a Professor, in 2012. His current research interests include array processing and smart antennas, wideband communications, cognitive radio, adaptive anti-jamming for satellite communications, satellite navigation, and date link systems.

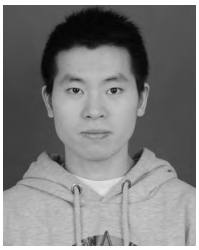

JIAN XIE received the M.Sc. and Ph.D. degrees from the School of Electronic Engineering, Xidian University, in 2012 and 2015, respectively. He is currently an Assistant Professor with Northwestern Polytechnical University. His research interests include antenna array processing and radar signal processing.